iJRASET
International Journal For Research in Applied Science and Engineering Technology

INTERNATIONAL JOURNAL FOR RESEARCH

IN APPLIED SCIENCE & ENGINEERING TECHNOLOGY

Volume: 11 **Issue:** VI **Month of publication:** June 2023

DOI: https://doi.org/10.22214/ijraset.2023.54531

www.ijraset.com

Call: 08813907089 | E-mail ID: ijraset@gmail.com

International Journal for Research in Applied Science & Engineering Technology (IJRASET)
ISSN: 2321-9653; IC Value: 45.98; SJ Impact Factor: 7.538
Volume 11 Issue VI Jun 2023- Available at www.ijraset.com

Performance Evaluation and Optimization of Solar Water Heater Systems: A Comprehensive Experimental Study

Pradeep Kumar[1], Amit Agrawal[2]
[1]*M.Tech Scholar,* [2]*Assistant Prof., Department of Mechanical Engineering, Shri Ram college of Engineering & Management Banmore Gwalior, Madhya Pradesh 476444, India*

Abstract: ***Solar water heaters are an efficient and sustainable technology for meeting the growing demand for hot water in residential and commercial applications. This abstract presents a comprehensive overview of the performance evaluation of solar water heater systems through an extensive experimental study. The study aims to assess the effectiveness and efficiency of different solar water heater configurations under varying operating conditions.***

The experimental investigation involved the measurement and analysis of key performance parameters such as solar collector efficiency, heat transfer efficiency, thermal storage capacity, and overall system efficiency. A range of factors including solar radiation intensity, ambient temperature, water flow rate, and collector tilt angle were systematically varied to examine their impact on system performance.

The results of the experimental study demonstrated the significant potential of solar water heaters in providing cost-effective and environmentally friendly hot water solutions. The solar collector efficiency was found to be highly influenced by the solar radiation intensity, with higher levels of solar irradiation leading to increased thermal energy generation. The heat transfer efficiency was optimized by adjusting the water flow rate and collector tilt angle, ensuring efficient transfer of heat from the collector to the water.

Furthermore, the thermal storage capacity of the system played a crucial role in maintaining a consistent supply of hot water during periods of low solar radiation or high demand. Overall system efficiency was found to be strongly dependent on the integration of efficient heat exchangers and insulation materials.

Based on the experimental findings, recommendations for system design and optimization were formulated, highlighting the importance of proper sizing, selection of suitable materials, and appropriate control strategies. The results also identified areas for future research, such as the integration of advanced heat transfer enhancement techniques and the utilization of hybrid solar water heater systems.

Keywords: Solar Water Heater, Performance Evaluation, Experimental Study, Solar Collector Efficiency, Heat Transfer Efficiency, Thermal Storage Capacity, System Efficiency.

I. INTRODUCTION

The sun harnesses its hydrogen atoms through fusion reactions, resulting in the generation of solar energy. These reactions produce highly energetic gamma rays, which, as a form of electromagnetic radiation, travel from the sun to the Earth, a distance of 150 million km. Among the different types of electromagnetic radiation, such as infrared, visible light, and ultraviolet, solar energy that reaches the Earth's surface can be directly captured through the use of photovoltaics (solar cells) and solar concentrators. Solar concentrators are employed to convert sunlight into heat energy, while photovoltaics generate electricity. Solar water heating technology relies on the utilization of solar energy collectors (concentrators) to convert radiation into heat energy [1]. A basic solar water heater typically consists of a flow path for the working fluid, a collector, and a storage tank.

Historical records indicate that the concept of a solar water heater (SWH) originated in the Roman Empire around 200 AD. The Romans used a simple method to heat their public baths, aiming to conserve coal and reduce labor by harnessing the principle of solar heating. Although these early devices were not fully self-sufficient, they laid the foundation for the development of solar water heating. Unfortunately, the idea of utilizing the sun for water heating was largely forgotten for over a thousand years following the fall of the Roman Empire. It was in the late 18th century that a Swiss naturalist named De Saussure reintroduced the concept of utilizing solar energy for water heating [2].

De Saussure constructed an insulated box with two glass panes, painting its bottom black to maximize solar radiation absorption. This design served as the prototype for all subsequent solar water heaters. De Saussure's experiments demonstrated that the interior of the insulated box reached temperatures higher than the boiling point of water when exposed to sunlight, thus illustrating the greenhouse effect for the first time. While De Saussure believed that his innovative mechanism would be valuable to scholars, it took more than a century for widespread recognition and adoption of solar water heating technology to occur.

II. SOLAR ENERGY POTENTIAL FOR WATER HEATING

The Earth receives a tremendous amount of solar energy in a single day, surpassing the total energy consumption of humanity. In comparison to the Earth's reserves of natural gas, coal, and oil, just 18 days of incoming solar radiation would yield a similar energy output. Beyond the Earth's atmosphere, there is an abundance of solar energy, with approximately 1,300 watts per square meter. However, when this energy enters the Earth's atmosphere, about one-third of it is reflected back into space, while the remaining portion continues towards the Earth's surface. On average, each square meter of the Earth's surface receives approximately 4.2 kilowatt-hours of solar energy per day [3].

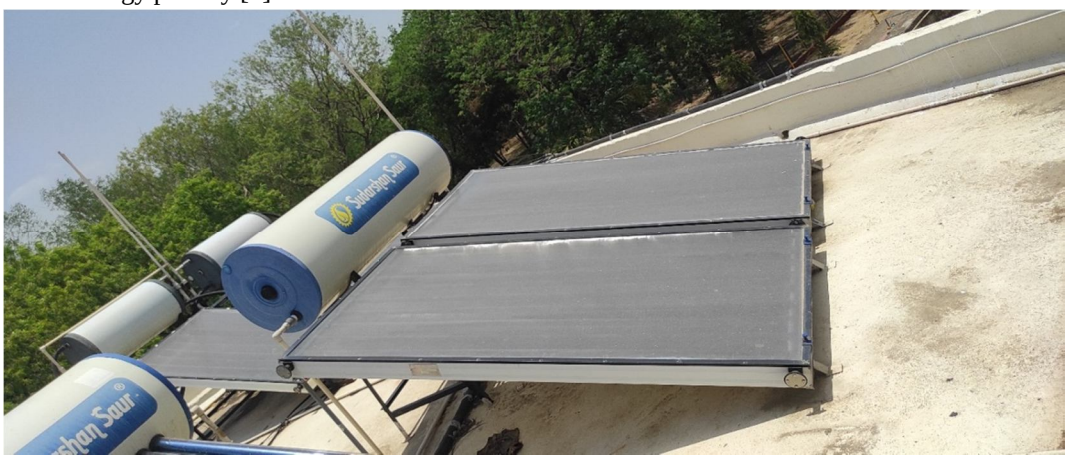

Fig.1: Setup of experimental solar water heater.

Scientists carefully monitor the levels of solar energy that reach specific regions at various times of the year. These measurements serve as a basis for estimating the amount of incident solar radiation in other locations with similar latitudes and climates. Solar energy measurements are typically presented in two forms: the total solar radiation on a horizontal surface or the total solar radiation on a surface that tracks the movement of the sun. These measurements allow researchers to quantify and compare the availability of solar energy across different geographical areas and climates.

A. Solar Insolation at System Site

The selection of a suitable geographical location is crucial when planning a solar-powered system. The performance of any solar system heavily relies on the amount of solar radiation, known as insolation, received at the site. Since insolation levels vary across different geographic locations, understanding the local meteorology is essential for designing an efficient solar system. In the case of city, it is situated in the northern region of the country, with latitude coordinates of 9.0765° N and 7.3986° E. Due to factors such as proximity to the Sahara Desert, the northern states of Nigeria generally experience higher levels of insolation [4]. This knowledge of regional insolation patterns helps in optimizing the design and performance of solar-powered systems in Abuja and similar locations.

B. Operating Principles of a SWH Based on the Thermosyphon Principle

When sunlight shines on the solar collector's transparent cover, the black-coated metallic plate within the collector absorbs the solar radiation as heat. This absorption of solar energy increases the internal energy of the metallic plate, causing the temperature of the solar collector to rise. The working fluid, which is closely connected to the black-coated metallic plate through a piping system, then absorbs this heat energy. As the working fluid absorbs the heat, it expands, leading to a decrease in its density. Based on the thermosyphon principle, gravity causes the colder fluid from the storage tank to flow into the collector, while the heated fluid rises naturally through the pipes at the top of the collector and returns to the storage tank.

ISSN: 2321-9653; IC Value: 45.98; SJ Impact Factor: 7.538
Volume 11 Issue VI Jun 2023- Available at www.ijraset.com

This process continues until the water in the storage tank reaches the desired temperature, with the hot water being transferred due to the increase in both volume and temperature. To control the temperature, the valves can be manually closed once the desired temperature is achieved, or the cycle can be regulated by a thermostat. A typical flat-plate collector, as illustrated in Figure 2, demonstrates this configuration.

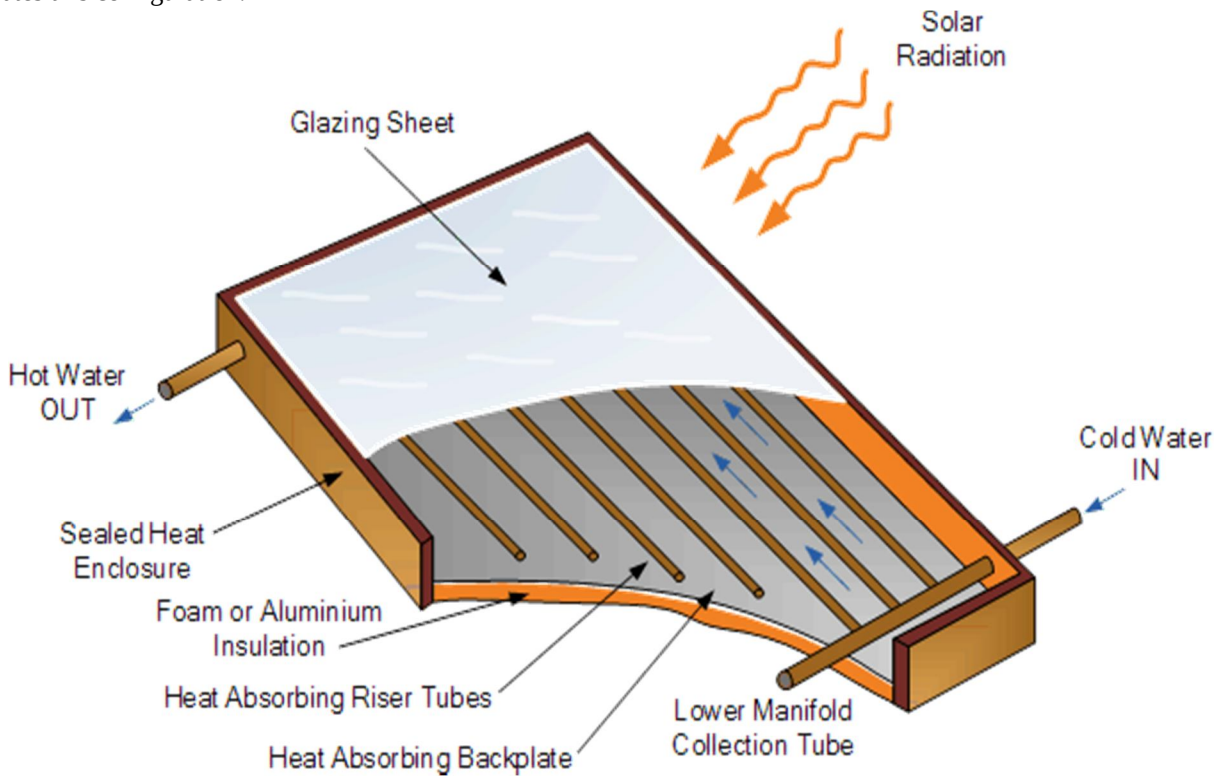

Figure 2: Typical flat-plate solar collector

C. Types of Solar Water Heating Systems

Solar water heating systems can be categorized as either passive or active, depending on how the heat transfer fluid is circulated within the system. The heat transfer fluid can be water or an antifreeze substance. In a passive system, the movement of water or the heat-absorbing fluid is achieved through natural convection and the force of gravity. This means that no electrical pump is required for fluid circulation within the system.

On the other hand, an active system utilizes an electric pump to facilitate the movement of the working fluid throughout the solar water heating system [6]. The pump actively circulates the heat transfer fluid, ensuring efficient heat transfer from the solar collector to the storage tank or point of use. This active circulation method provides greater control over the flow rate and enables the system to operate effectively even in situations where natural convection is limited.

Both passive and active systems have their advantages and considerations, and the choice between them depends on factors such as system size, efficiency requirements, and the specific conditions of the installation site.

D. Experimentation of the Solar Water Heater

The SWH was created and dimensioned in a way that made it possible to choose materials that met the requirements of the design. The flow channel, storage tank, and flat-plate collector are the main elements taken into account throughout the design phase [7].

E. Experimental Assumptions

The SWH was designed and dimensioned using the following presumptions:

1) The flow is laminar and evenly dispersed inside the tubes.
2) The collector has a uniform radiation incidence.
3) The following numerical parameters are taken into account when designing and sizing the system.

F. Testing Setup

The solar water heater may be shown in Figure 3.8. The collector is inclined towards the horizontal plane at an angle of 9o. The apparatus is pointed south wise for the testing because India is in the northern hemisphere. On three different days, from 10 am to 3 pm, the ambient temperature, as well as the entrance and outflow temperatures from the collector, were all monitored hourly. It should be mentioned that the test period was extended by persistent rain. The volume of flow per minute was measured using a timer and a calibrated container to calculate the flow rate. Following several attempts, an average value of 0.15 litres per minute was obtained. From the website, data on solar irradiance for the time period was also collected.

1) The solar water heater was placed facing south during the testing period to receive solar energy.
2) Water was then added to the storage tank using the buffer tank's flexible lines.
3) The attached thermometers provided the initial intake and exit temperature data, and the surrounding temperature was recorded.
4) The input valve of the collector was opened to start the cycle.
5) Step 3 was repeated every hour until the heating session was over.

III. RESULTS

The data required to analyses the performance of the SWH is displayed below. Over the course of two sets of three separate days, the investigations were conducted. throughout the early wet season of the first set and the dry season of the second set.

Using a model solar water heater, the average flow rate of 0.0025 kg/s and the other measurements taken throughout the test were used to calculate the instantaneous system efficiency for each set of data by Equation [8].

Table 1 Readings for the first day of experiments sample water heater (23/09/22 readings)

Time(h)	Ambient Temp. (^{0}C)	Inlet Temp (^{0}C)	Outlet Temp (^{0}C)	IrradianceW/m^2	Efficiency(%)
10:30	25.00	25.00	27.10	567	5.12
11:30	26.00	30.00	30.70	602	1.60
12:30	26.00	30.20	31.30	709	2.15
13:30	27.00	30.10	50.20	822	33.79
14:30	27.20	32.00	55.50	683	47.53
15:30	28.00	30.40	47.70	546	43.77

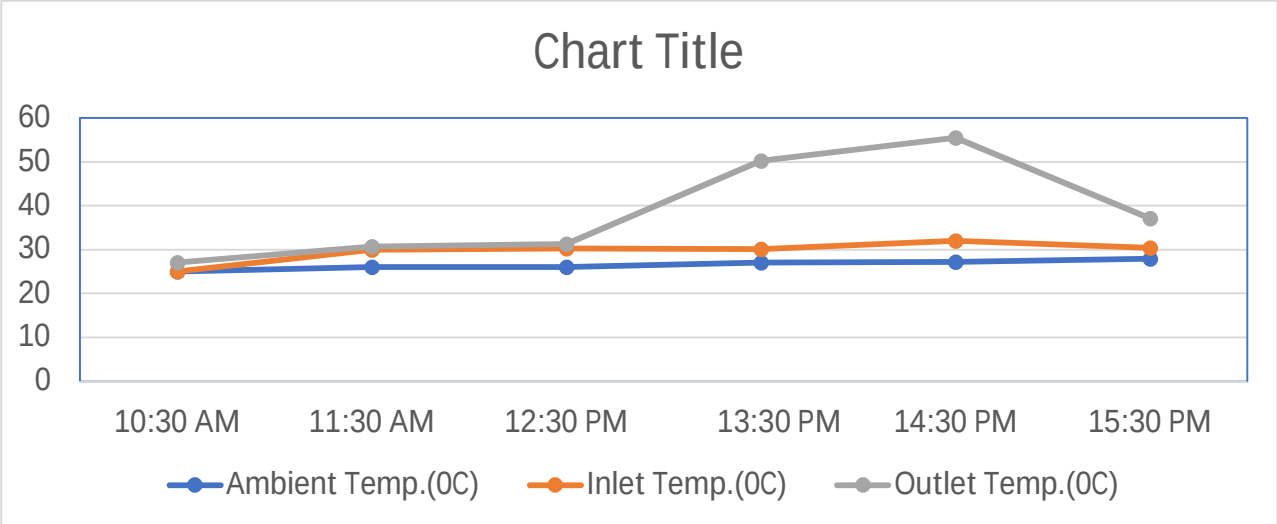

Graph 1: Temperature against efficiency for day one

Graph 1 shows that the using simple solar water heater outlet temperature climbs gradually for the first few hours, then rapidly from midday until it reaches its peak at two in the afternoon. It's crucial to remember that the output temperature peaks one hour before the irradiance levels peak. According Table 1, the output temperature peaks right when efficiency is at its best. It may be inferred that the efficiency and the outflow temperature are closely related [9].

Figure 3: experiments setup water heater with glass cover.

Table 2 Readings for concrete floor materials the second day of experiments (25/09/22 readings).

Time (h)	Ambient Temp. (^{0}C)	Inlet Temp (^{0}C)	Outlet Temp (^{0}C)	Irradiance W/m^2	Efficiency (%)
10:30	27.00	26.20	28.20	522	5.29
11:30	27.00	26.60	47.80	610	48.06
12:30	29.00	27.20	54.00	625	59.24
13:30	29.10	27.40	50.00	740	42.19
14:30	30.00	30.20	60.00	660	62.38
15:30	30.10	32.20	53.00	469	61.27

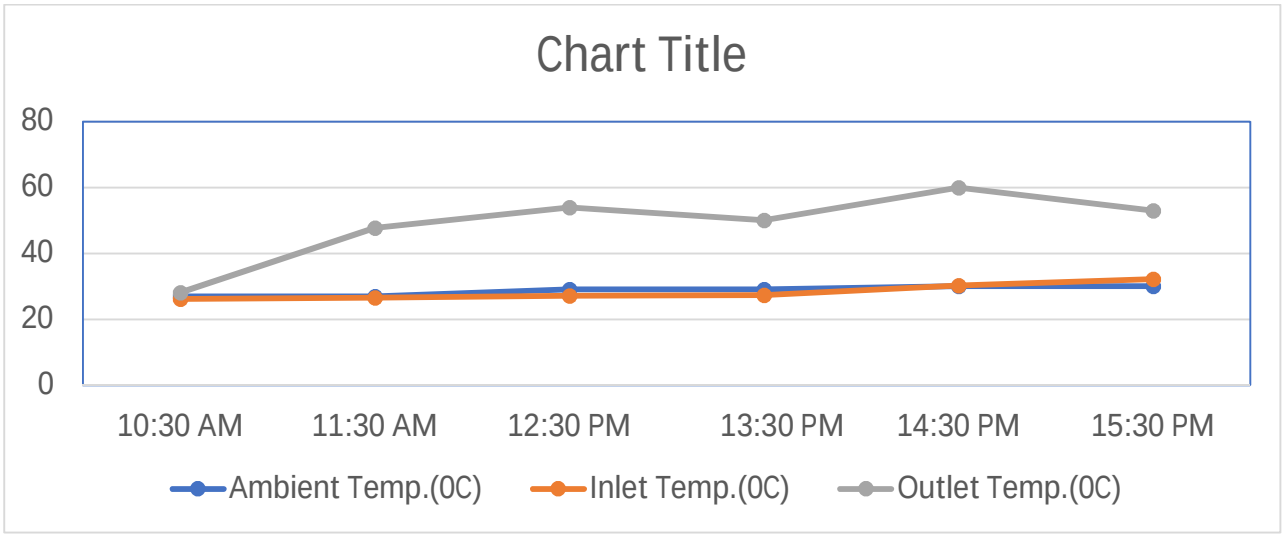

Graph 2: Temperature against efficiency for day two.

A comparable gradient between the input temperature and the ambient temperature is shown using the concrete flower and solar water heater in Graph 2, up until the irradiance peak. At that point, the input temperature starts to gradually rise while the ambient temperature starts to drop. The irradiance levels peak an hour before the outlet temperature, just like on the first day of testing. As seen in Table 2, the system efficiency exhibits a similar trendline to the output temperature. The maximum efficiency decreased from day one to day two [10].

Table 3 Readings for Charcoal material the third day of experiments (01/10/22 readings)

Time(h)	AmbientTemp. (^{0}C)	Inlet Temp(^{0}C)	Outlet Temp (^{0}C)	IrradianceW/m^2	Efficiency(%)
10:30	25.50	23.10	24.50	384	5.04
11:30	26.40	24.20	42.00	370	66.46
12:30	27.30	24.70	48.00	549	58.63
13:30	28.10	25.40	57.00	631	69.18
14:30	28.30	27.30	53.30	560	54.14
15:30	29.00	30.00	50.00	545	50.70

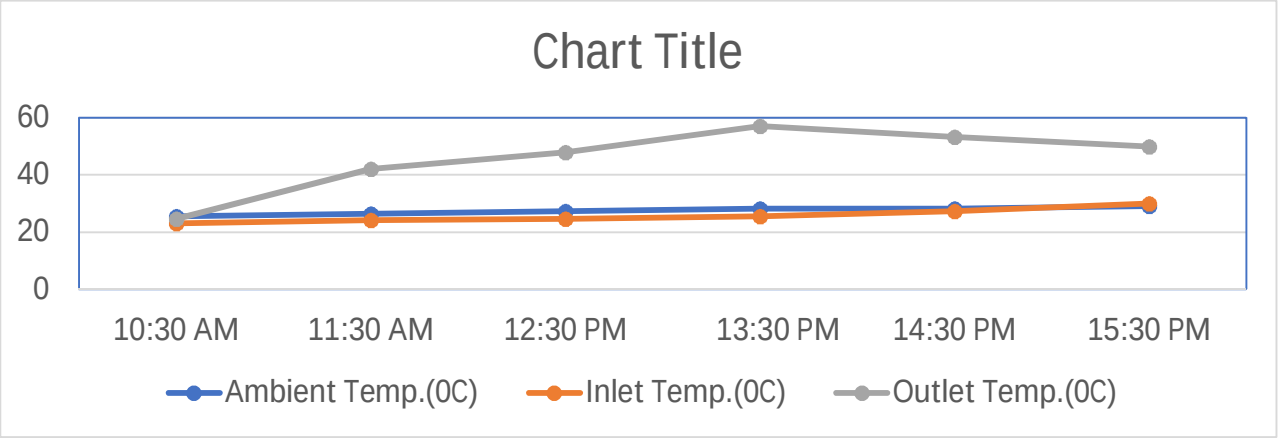

Graph 3: Temperature against efficiency for day three

Graph 3 reveals that, in contrast to the find the using charcoal particles with concrete flower base solar water heater, in the outlet temperature and irradiance levels peak at the same time. At one o'clock in the afternoon, when irradiance levels peaked the first two days, this happens. The ambient temperature rises steadily until one o'clock in the afternoon and then remains constant throughout the day as the inlet temperature does. Table 3 shows that, even as the output temperature rises, efficiency somewhat decreases between eleven am and twelve pm. The efficiency then increases from twelve to one, when it reaches its apex.

Table 4 Readings for Nano particle silica the fourth day of experiments (28/10/22 readings)

Time(h)	AmbientTemp. (^{0}C)	Inlet Temp(^{0}C)	Outlet Temp (^{0}C)	IrradianceW/m^2	Efficiency(%)
10:30	29.10	27.80	31.30	810	5.97
11:30	30.00	28.70	51.10	902	34.30
12:30	32.10	30.50	72.40	935	61.91
13:30	32.50	35.70	65.50	850	48.43
14:30	33.00	41.90	59.80	720	34.35
15:30	33.20	44.10	53.00	510	24.10

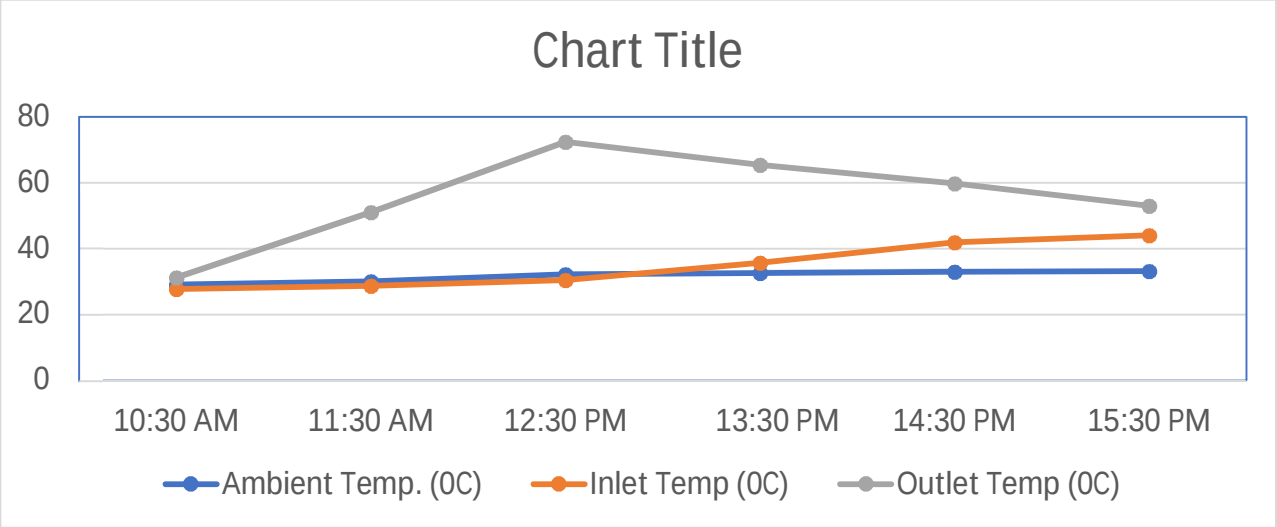

Graph 4: Temperature against efficiency for day four.

Graph 4 demonstrates a considerable with nano silica particles with concrete flower, base solar water heater rise in irradiation levels from the first three testing days. The irradiance is shown to peak at noon as opposed to the values from day one to day three. In addition, the outlet temperature peaked at twelve o'clock and rose above data from the previous three days. Table 4 makes clear that there is a strong correlation between efficiency and output temperature since they both peak at the same time. The slopes of their climb and descent are comparable. This is consistent with the pattern seen on days one and three.

Table 5 Readings for Black carbon material the fifth day of experiments (29/10/22 readings)

Time(h)	AmbientTemp. (^{0}C)	Inlet Temp(^{0}C)	Outlet Temp (^{0}C)	IrradianceW/m^2	Efficiency(%)
10:30	29.10	28.70	30.50	828	3.01
11:30	29.50	34.30	51.10	900	24.71
12:30	31.00	37.80	74.00	908	55.08
13:30	31.30	43.60	61.50	810	31.53
14:30	32.21	46.50	61.30	650	31.45
15:30	32.20	46.70	56.60	430	31.80

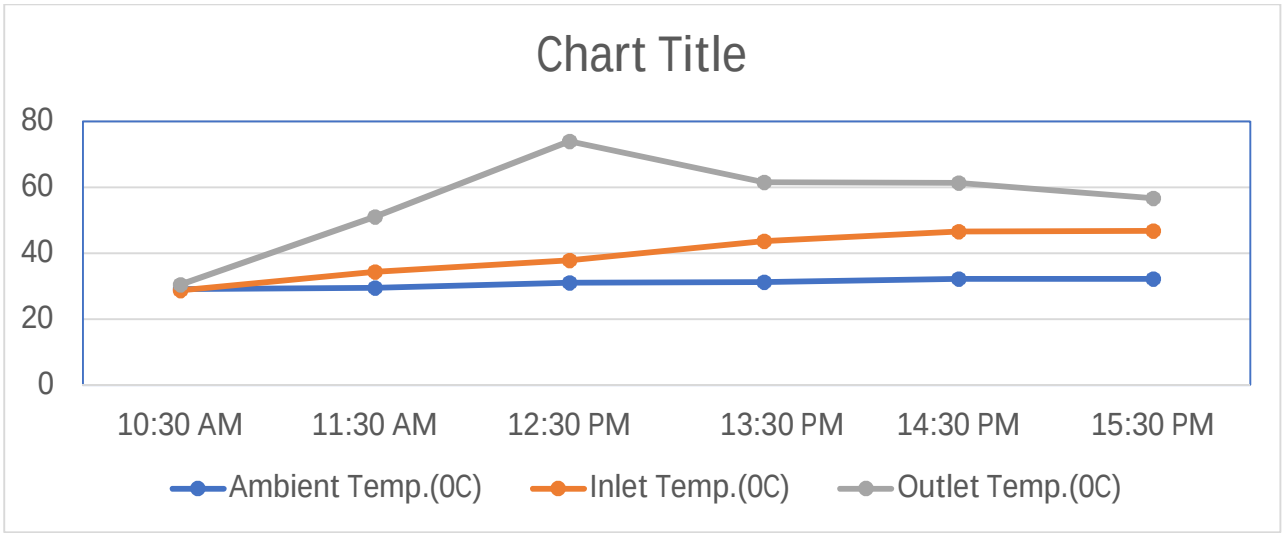

Graph 5: Temperature against efficiency for day five

Graph 5 for day five demonstrates in that a using black carbon material, silica with concrete floor base, solar water heater in the irradiance increases between ten and eleven in the morning, remains steady until twelve, and then progressively decreases. This pattern differs significantly from those shown on test days prior. Similar to day four, the outlet temperature peaks around twelve o'clock. Efficiency and output temperature both peak at the same time and have comparable trendlines, as shown in Table 5. This demonstrates a connection to the day four findings.

Table 6 Readings for Mixture particles the sixth day of experiments (30/10/22 readings)

Time(h)	AmbientTemp. (^{0}C)	Inlet Temp(^{0}C)	Outlet Temp (^{0}C)	IrradianceW/m^2	Efficiency(%)
10:30	30.20	30.40	35.20	820	8.08
11:30	32.00	30.70	60.80	922	45.10
12:30	34.00	39.20	77.30	936	56.23
13:30	35.00	41.00	74.50	876	52.83
14:30	35.00	42.10	64.70	740	42.19
15:30	36.00	44.40	61.40	542	44.09

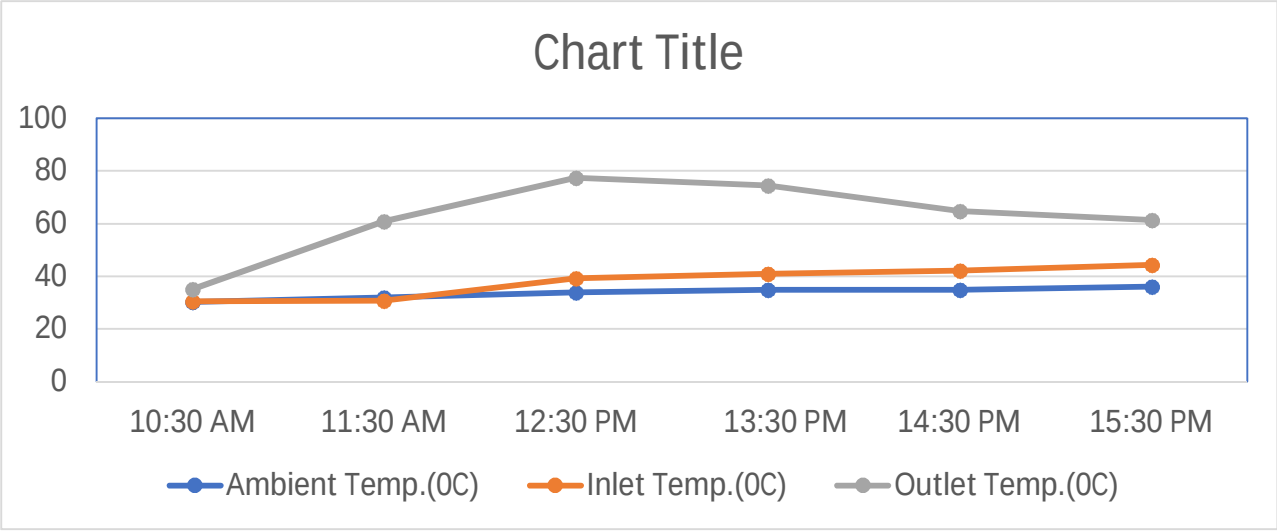

Graph 6: Temperature against efficiency for day six.

Graph 6 shows at midday, now black carbon material, charcoal, concrete floor with nano particles in solar water heater the outflow temperature peaks at 77.3^{0}C. When compared to the testing days before, this is the largest number of observations. As was the case on days four and five, the irradiance levels peak at midday. The connection between efficiency and output temperature in Table 6 is comparable to that of days four and five. The highest efficiency recorded during the tests on the previous day was 56.23 %.

Table 7 Mixture to Outlet temperature for the six days of testing.

Time(h)	Day One	DayTwo	Day Three	DayFour	DayFive	Day Six
10.30	27.10	28.20	24.50	31.30	30.50	35.20
11:30	30.70	47.80	42.00	51.10	51.10	60.80
12:30	31.30	54.00	48.00	72.40	74.00	77.30
13:30	50.20	50.00	57.00	65.50	61.50	74.50
14:30	55.50	60.00	53.30	59.80	61.30	64.70
15:30	47.70	53.00	50.00	53.00	56.60	61.40

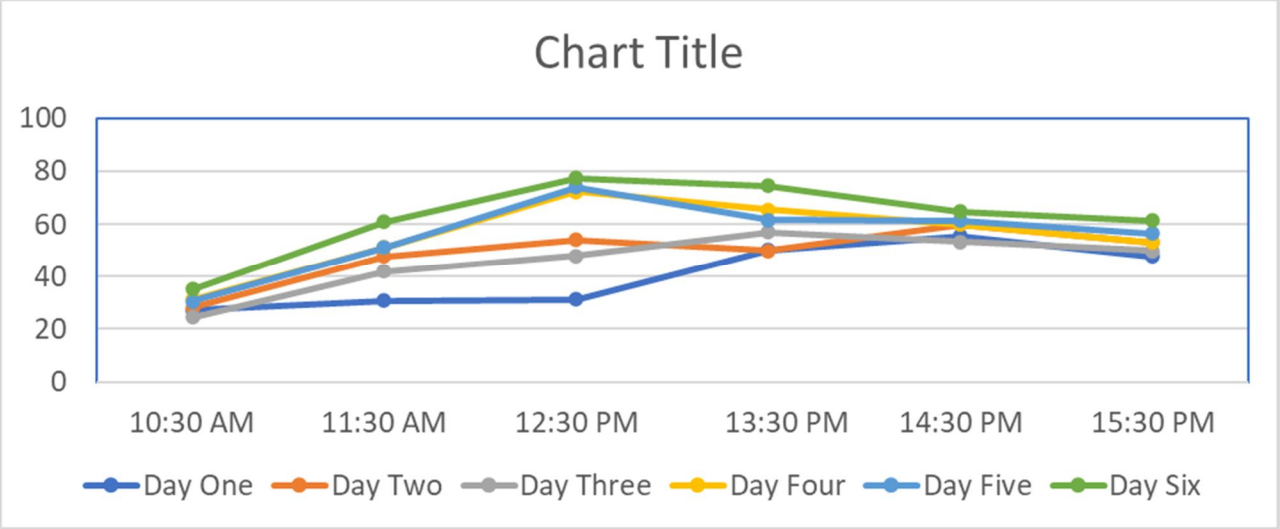

Graph 7: Outlet temperature for the six days of testing.

When comparing to the using of simple water heater, carbon materials, concrete floor, or nano particles outlet temperatures for days one through three to those for days four through six, graph 7 reveals a sizable variation. Day one through three of the testing took place in the late rainy season, whereas days four through six were conducted during the dry season. For days one through three, the peak outflow temperature was between one and two in the afternoon, whereas for days four through six, the highest was at midday. There is no doubt that the system works better during the dry season.

IV. DISCUSSION OF RESULTS

The overall results reveal that the utilization of a combination of nanoparticles, black carbon material, and a concrete floor yielded the most favorable performance across all experiments, establishing a robust association between the output temperature and irradiation levels. The highest recorded outlet temperature during the initial three days of testing in the late rainy season was 57.00 0C. Similarly, the maximum outflow temperature observed during the final three days of testing in the dry season reached 77.3 0C. This unequivocally demonstrates the superior functionality of the system during dry conditions. The system was designed with a target output temperature of 70 0C, and a collector area of 0.76 m2 was employed in the design process, as mentioned in previous works. The system successfully heated a total of 36 liters of water. However, it fell short of the goal of supplying 75 liters of water at 60 °C daily.

In comparison, another study based on their design requiring a collector area of 1.464 m2 achieved a maximum output temperature of 77.3 0C on a surface area of 2.3 m2. Despite their larger collector area, their peak outlet temperature was slightly lower than the highest value observed in this study, highlighting the influence of both collector area and site irradiance on system performance. The sixth day of testing recorded the highest irradiation level of 936 W/m2, coinciding with the maximum outflow temperature of 77.3 0C. The most significant increase in outflow temperature occurred between 13.30 am and noon on the fourth day, with a rise of 75.5 0C. Notably, day three exhibited the lowest irradiance levels. Based on the collected data, the system demonstrated its optimal performance on day four, achieving an efficiency of 69.18%.

V. CONCLUSION

Upon conducting the experiments, the outcomes are as follows. In the initial three days of testing during the late rainy season, the highest recorded outflow temperature reached 57.00C. Conversely, during the final three days of testing in the dry season, the maximum outflow temperature measured was 77.3 0C. It is evident from this comparison that the system performs more efficiently in the dry season when the irradiance levels are higher. The highest irradiance level observed during the sixth day of testing was 936 W/m2, and the system achieved a peak efficiency of 69.18%. The overall findings indicate that the combination of a mixture of nanoparticles and black carbon material with a concrete floor yielded the best performance throughout the experiments. This highlights a strong correlation between the output temperature and irradiation levels. Although the system fell short of the target of supplying 75 liters of water at 60°C daily, it successfully heated a total of 36 liters of water.

In comparison to another study that utilized a collector area of 1.464 m², our system with a collector area of 0.76 m² achieved a slightly higher maximum output temperature of 77.3°C. This emphasizes the influence of both collector area and site irradiance on system performance. Notably, the highest irradiation level of 936 W/m² coincided with the maximum outflow temperature of 77.3°C on the sixth day of testing. The most significant increase in outflow temperature occurred between 13.30 am and noon on the fourth day, with a rise of 75.5°C. Day three exhibited the lowest irradiance levels. Based on the collected data, the system demonstrated its optimal performance on the fourth day, achieving an efficiency of 69.18%.

VI. FUTURE PERSPECTIVES

Considering the limitations in terms of time and resources, the following recommendations are proposed to enhance the system testing and performance:

1) Incorporate a sensor to monitor water levels and regulate the flow accordingly.
2) Install a flow meter to easily measure the flow rate of the working fluid.

REFERENCES

[1] Abdunnabi, M., Rohuma, I., Endya, E., & Belal, E. (2018). Review on solar water heating in Libya. https://www.researchgate.net/publication/329845152_Review_on_solar_water_heating_in_Libya/figures?lo=1
[2] Adefarati, T., & Bansal, R. C. (2019). Energizing Renewable Energy Systems and Distribution Generation. In Pathways to a Smarter Power System (pp. 29–65). Elsevier. https://doi.org/10.1016/b978-0-08-102592-5.00002-8
[3] Alternative Energy Tutorials. (2015). Solar Flat Plate Collectors for Solar Hot Water. http://www.alternative-energy-tutorials.com/solar-hot-water/flat-plate-collector.html
[4] API Energy. (n.d.). Active Vented System. Retrieved September 29, 2020, from https://apienergy.co.uk/product/active-vented-system-drain-back-solar-water-heating-system/
[5] Atia, D. M., Fahmy, F. H., Ahmed, N. M., & Dorrah, H. T. (2012). Optimal sizing of a solar water heating system based on a genetic algorithm for an aquaculture system. Mathematical and Computer Modelling, 55(3–4), 1436–1449. https://doi.org/10.1016/j.mcm.2011.10.022
[6] Azom. (2005). Aluminium Specifications, Properties, Classifications and Classes. https://www.azom.com/article.aspx?ArticleID=2863
[7] Barry, C. (2018). thermal properties of glass fiber thread. B&W FIBERGLASS NEWS, 1. http://info.bwfiberglass.com/blog/the-thermal-properties-of-glass-fiber-thread
[8] Dean, J. (n.d.). Domestic Hot Water Assessment Guidelines (Fact Sheet), Saving Energy In Commercial Buildings, NREL (National Renewable Energy Laboratory). Retrieved May 19, 2020, from https://www.nrel.gov/docs/fy11osti/50118.pdf
[9] Eagle Stainless. (n.d.). Characteristics of Stainless Steel. Retrieved September 27, 2020, from https://eagletube.com/about-us/news/stainless-steel-characteristics/
[10] Ekpo, J., & Enyinna, P. (2017). Design and Construction of a Solar Water Heater for Environmental Sustainability. British Journal of Applied Science & Technology, 20(3), 1–15. https://doi.org/10.9734/bjast/2017/31820

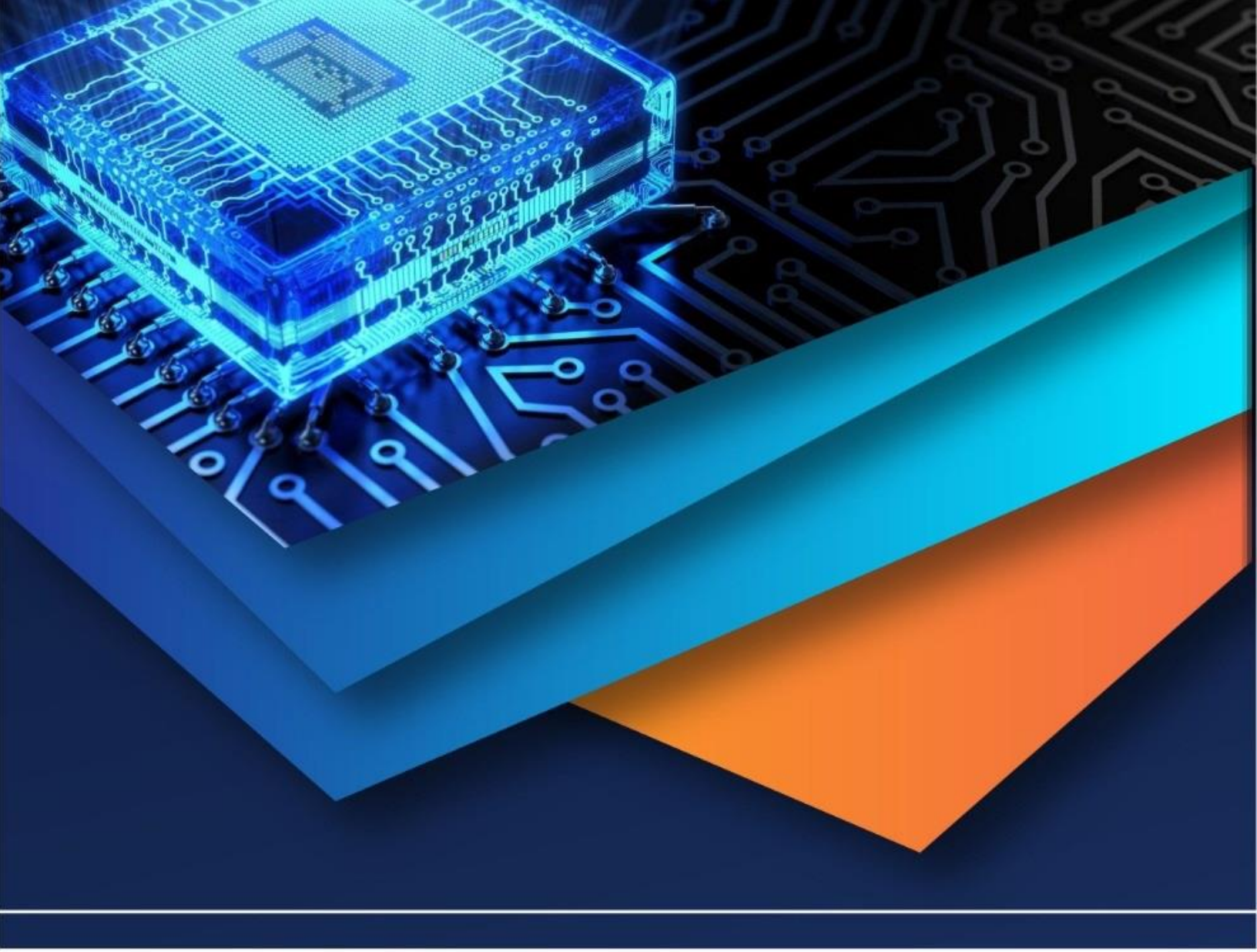

10.22214/IJRASET

45.98

IMPACT FACTOR: 7.129

IMPACT FACTOR: 7.429

INTERNATIONAL JOURNAL FOR RESEARCH

IN APPLIED SCIENCE & ENGINEERING TECHNOLOGY